SSRG International Journal of Electronics and Communication Engineering
ISSN: 2348-8549/ https://doi.org/10.14445/23488549/IJECE-V11I7P109

Volume 11 Issue 7, 89-97, July 2024

Original Article

Deep Residual Network and Water Cloud Model-Based Soil Moisture Retrieval Using Satellite Images

Sanjay B. Waykar[1], Rajesh Kadu[2], Amitkumar Manekar[3]

[1,2]*Department of IT, Mahatma Gandhi Mission's College of Engineering & Technology, Maharashtra, India.*
[3]*Department of IT, Shri Sant Gajanan Maharaj College of Engineering Shegaon, Maharashtra, India.*

[3]*Corresponding Author : asmanekar24@gmail.com*

Received: 07 May 2024 Revised: 07 June 2024 Accepted: 06 July 2024 Published: 27 July 2024

Abstract - *Soil moisture is a critical part of the link between land carbon cycle and surface-ground water motion. It also is vital in energy exchange between land/atmosphere; furthermore, soil moisture is an important determinant process for plant growth and productivity. By making the technique use satellite imagery, it is able to predict soil moisture content more accurately rather than using vegetation indices like the "Wide Dynamic Range Vegetation Index (WDRVI), Simple Ratio (SR), or Green Leaf Area Index (GLAI)". A Deep Residual Network (DRN)-based "water cloud model "for soil moisture" forecasting is generated according to the vegetation indices. Additionally, soil moisture is derived using vegetation indices such as the "Wide Dynamic Range Vegetation Index (WDRVI), Simple Ratio (SR), and Green Leaf Area Index (GLAI)". Performance of the developed DRN-based "water cloud model "was also evaluated in terms of RMSE and estimation error. The objective of this research work is to come up with a new modeling approach of soil moisture retrieval by improving "water cloud model "with satellite images and vegetation indices in one hand, and consequently to verify its performance through the application of Deep Residual Network (DRN)-based "water cloud model "on another hand. According to the experimental results, the suggested DRN-based "water cloud model "performed better than the others, with the smallest estimate error and Root Mean Square Error (RMSE) values of 0.523 and 0.69, respectively. The developed method's estimation error is lower than that of the Semi-Empirical Water Cloud Model, Deep Multi Model Fusion Network, Genetic Algorithm (GA), Convolution Neural Network and Regression (CNNR), and Particle Swarm Optimization (PSO), respectively, at 94.14%, 65.32%, 91.63%, 63.12%, and 91.10%. The developed scheme's RMSE is lower than that of the CNNR, PSO, Genetic Algorithm GA, Deep Multi Model Fusion Network, Semi Empirical Water Cloud Model, and 93.52%, 90.33%, 93.11%, and 89.72%, respectively.*

Keywords - *Soil moisture, Satellite images, Water cloud model, Deep residual network, Vegetation index.*

1. Introduction

One of the main variables influencing our climate is soil moisture, which is defined as the amount of water in the unsaturated zone of the soil. Through plant transpiration and soil evaporation, soil moisture impacts the water, biogeochemical, and energy cycles between the land and the surface [7]. Since soil can record the various incidents that have occurred in the past, it can be used in the prediction of floods, heat cycles, thunderstorms, and droughts [8]. Moreover, it is regarded to be a significant parameter in research carried out for the analysis of slope stability and water balance [9]. Furthermore, soil moisture has a high significance as it forms an essential link connecting life with the hydrological cycle. Along with surface temperature, it is also essential in defining wind patterns, circulation, and the depth of the planetary boundary layer [10]. Therefore, it is critical to forecast the soil moisture content in order to examine the impact of soil moisture on the many aspects mentioned above. Traditionally, the very precise in-situ techniques are used to assess soil moisture. But, these approaches are not cost-effective and only cover a limited area [11]. The information obtained from satellites can be used to estimate soil moisture on a large scale [10].

The use of satellites opened a new era of soil moisture measurement techniques, which make use of the reflectance at the soil surface depending on the moisture. Visible, microwave and infrared rays are employed in soil moisture retrieval systems using satellite data [11]. For the purpose of ensuring food security and tracking crop growth and yields, effective estimation of soil moisture requires both spatial and temporal resolution. Vegetation is another significant factor affecting soil moisture since it can draw moisture out of the soil [12]. The reflectance property of the soil is used to calculate soil moisture, but this is insufficient because soil irradiance fluctuates with time and is dependent on meteorological conditions [21, 28]. By taking into account the information from two or more spectral bands and merging

them to create the Vegetation Index (VI), this can be prevented [13, 18, 19]. Plant physiological and biophysical characteristics can be observed using the vegetation index that is calculated using satellite data [14]. Numerous vegetation indices, including the Fraction of Photosynthesis Active Radiation (FPAR) [14], Soil-Adjusted Vegetation Index (SAVI), Normalized Difference Vegetation Index (NDVI), and Temperature Vegetation Dryness Index (TVDI) [9, 15, 18], facilitate the estimation of soil moisture.

Soil moisture [25, 26] is a highly crucial aspect that impacts the respiration of soil microbes, disease spreading, groundwater runoff, plant growth and productivity, surface temperature, and so on. It is also crucial for modeling various hydrological processes since it regulates the exchange of energy and water between the atmosphere and the ground. Accurately providing data on soil moisture dynamics is essential for planning and managing water resources, agricultural productivity, climate forecast, and flood disaster monitoring [7]. However, soil moisture is difficult to estimate since it is very nonlinear and inconsistent over time and space. An advantageous technique for modeling soil moisture dynamics is deep learning [20, 25]. The advancement of deep learning algorithms in recent years has made it possible to anticipate the spatiotemporal elements that affect soil moisture. Since deep learning algorithms provide a balance between retrieval accuracy and processing speed, they are frequently employed in real-time applications [15, 18].

Here, a DRN-based "water cloud model "is developed for estimating soil moisture. The DRN-based "water cloud model "utilizes vegetation indices, such as GLAI, SR, and WDRVI for performing soil moisture retrieval. The vegetation indices are extracted from the input images captured using satellites [27, 29].

1.1. Contribution

The contribution of the research is given below:

1.1.1. DRN-based Water Cloud Model

To efficiently carry out soil moisture retrieval, a unique DRN-based "water cloud model "is created. To estimate soil moisture, the DRN uses the vegetation indices collected and the backscattering coefficient computed by the water cloud model. The study's remaining section is structured as follows: Section 2 reviews pertinent works on soil moisture retrieval. Section 3 delves deeper into the established DRN-based "water cloud model," while Section 4 evaluates its effectiveness in retrieving soil moisture. Section 5 concludes the paper and offers future directions.

2. Literature Survey

Several works have been performed to estimate the amount of soil moisture content. Tsagkatakis G. et al. [1] proposed a Genetic Algorithm (GA) optimization technique for estimating soil moisture, which successfully calculated unbiased estimates even in the presence of noise [24]. The state provided a semi-empirical "water cloud model" for predicting soil moisture, set al. in [2], where data from a sizable area was obtained [23]. The approach correctly calculated the crop-covered backscatter coefficient using the vegetative indices; however, multi-polarization was not considered to guarantee the practical implementation of the method. Tsagkatakis created a Deep multi-model fusion network, G. et al. [3] to extract soil moisture from the surrounding environment. The approach did not take land cover information into account, which could have decreased the predicted value of soil moisture, even though it produced high-quality soil moisture estimation with a low estimation error rate [22].

Restoring soil moisture is crucial for managing agricultural practices and understanding the relationship between the land and the atmosphere. Advances in machine learning and remote sensing have brought about changes in traditional methods. Convolution Neural Networks (CNNs) were used by Zhang et al. [30] to estimate soil moisture using satellite imagery, and their findings demonstrated increased accuracy over traditional techniques. Liu et al. [31] improved soil moisture content prediction by combining vegetation indexes and machine learning techniques. Recent developments in Deep Residual Networks (DRNs) by Kim et al. demonstrated notable increases in model robustness and accuracy. By combining DRNs with the water cloud model, this work makes use of these advancements to enhance soil moisture retrieval using satellite imagery. The impact of vegetation cover was considered in the CNNR model [4] developed by Liu J et al. The CNNR model achieved high accuracy of soil moisture retrieval; however, it considered only dual polarized data of sentinel 1. Mohsen Jamali et al. [20] implemented a model for identifying wheat leaf diseases based on Vegetation Indices (VIs). Here, the Deep Neural Network (DNN) offered valuable insights into the management of crops with good spatial and temporal accuracy using satellite imagery [21, 28]. However, some important features are not considered.

3. Proposed Method

Soil moisture retrieval is highly significant in forecasting the growth of plants and their productivity, thereby ensuring food security [17]. Here, a successful "water cloud model "based on DRN is created to estimate soil moisture. The below steps will help set up the suggested DRN-based water cloud model. Initially, take images from the datasets hosting satellite images. Following their acquisition, the input photographs undergo additional processing that aids in the determination of the vegetation index and the "water cloud model." Following this, additional indices such as GLAI, SR, and WDRVI are extracted, and the backscattering coefficient is obtained by considering the water cloud model. In order to assess the moisture content, the calculated indices and backscattering

coefficient are sent to the DRN for soil moisture retrieval. Figure 1 illustrates the operational diagram for the DRN-based water cloud model. The subsequent sub-sections outline each stage of this process in detail". There are three stages to the suggested soil moisture retrieval process: using vegetation indicators (WDRVI, SR, and GLAI) and satellite photos to gather preliminary data. "Developing a model of water cloud with the use of Deep Residual Networks (DRNs) on such data. For the assessment of this model performance, utilization of estimator error measures and Root Mean Square Error (RMSE) formulas".

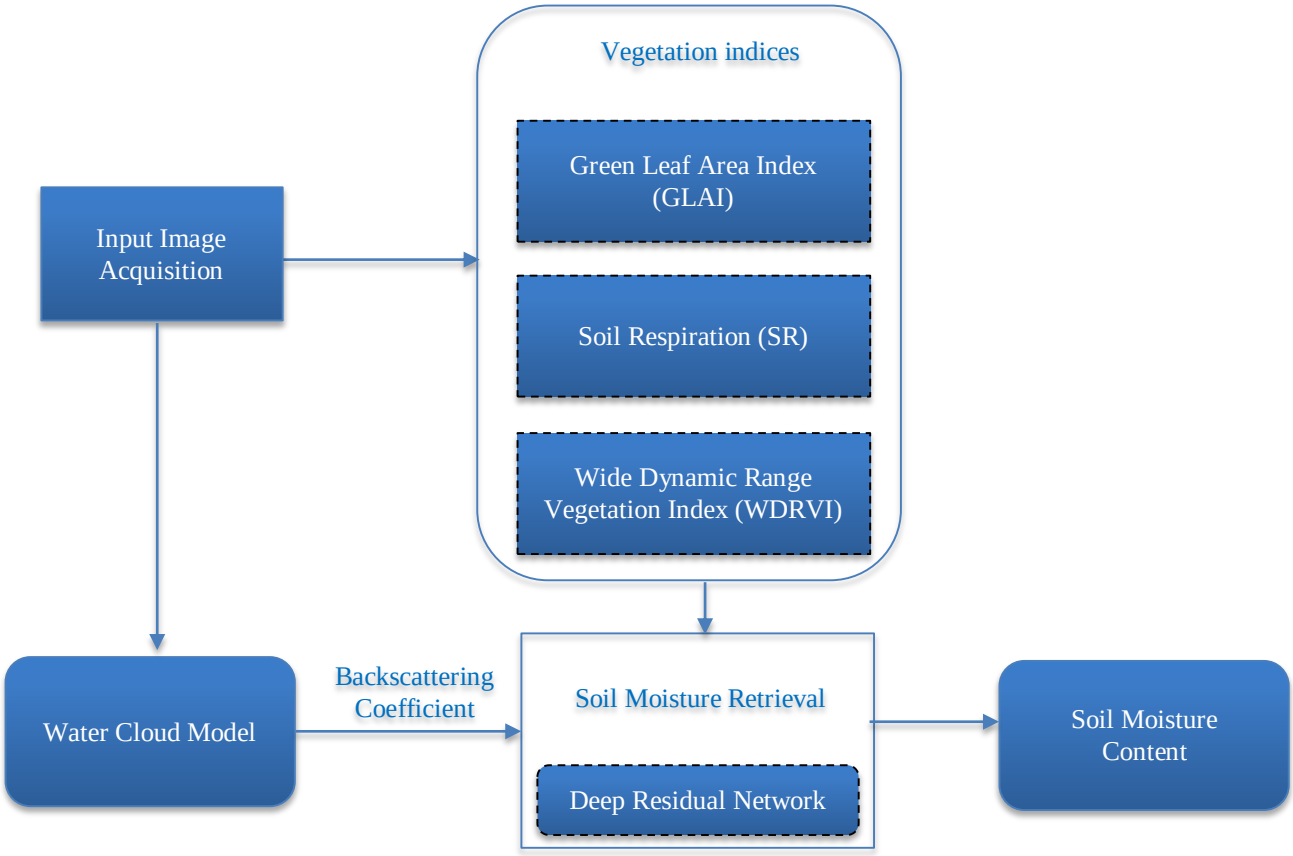

Fig. 1 Schematic view of the devised DRN-based water cloud model

3.1. Image Acquisition

The process of retrieving soil moisture involves taking into account the satellite photos that were taken. Thus, the information gathered from satellites provides the spatial content needed to estimate ecological function, canopy cover, land use, and other factors. let us Consider a dataset F containing a total of m satellite images, which is given by the following expression,

$$F = \{f_1, f_2, .., f_k, .., f_m\} \quad (1)$$

Here, $1 \leq k \leq m$ and f_k denotes the k^{th} image, which is utilized for estimating the soil moisture content.

3.2. Extraction of Vegetation Index

Vegetation indices have the following benefits: they can monitor vegetation over time, cover huge areas, and combine index data with other data sources. The image f_k is subjected to the vegetation index extraction step, where the significant features, such as GLAI, SR, and WDRVI [17], are extracted. The spectral bands are transformed to compute the vegetation index so that the green plants in the pixel appear distinctly. Vegetation indices give the amount of greenness contained in the pixel of the image and are used to quantify the vegetation strength contained in the pixel. The following subsection briefs the vegetation indices used in this research.

3.2.1. Green Leaf Area Index (GLAI)

The crop growth and development rates determine the amount of solar radiation that is shielded from the crop by the crop GLAIs. Besides, it is useful in determining the plant's life cycle physiology, such as transpiration, yield and productivity in relation to photosynthesis. GLAI can be described as the proportion of the area of the leaf to the ground area and can be represented as,

$$v_1 = 3.618 \times b - 0.118 \quad (2)$$

Where, b denotes the Enhanced Vegetation Index (EVI) feature.

3.2.2. Simple Ratio (SR)

SR, also known as the Ration "Vegetation Index (RVI)", is defined as the ratio of Near InfraRed (NIR) to the red band. By efficiently lowering the transmittance, SR lessens the effect of the atmosphere on plants. SR can be written as,

$$v_2 = \frac{\alpha}{\beta} \tag{3}$$

Here, α represents the NIR and βsignifies the red band.

3.2.3. Wide Dynamic Range Vegetation Index (WDRVI)

WDRVI is employed for increasing the sensitivity of NDVI, which is used to map the spatial and temporal distributions of any vegetation. It is given by,

$$v_3 = \frac{0.5\times\alpha-\beta}{0.5\times\alpha+\beta} \tag{4}$$

The vegetative indices obtained $\{v_1, v_2, v_3\}$are subjected to DRN, which $v_1$represents the GLAI, $v_2$signifies the SR, and $v_3$denotes the WDRVI.

3.3. Water Cloud Model

We require the "water cloud model", as mentioned in the previous study, in order to calculate the backscattering coefficient of the soil surface in saline areas with vegetation cover. Indicators of soil condition such as salinity, roughness, vegetation, and soil humidity content affect this coefficient.

Hence, the need to eliminate the impact of vegetation when one calculates for the backscattering coefficient. This "water cloud model "is based on two ideas:

(i) Disregarding the fact that the earth's surface and trees lead to multiple scattering, and
(ii) Uniformity in a canopy layer. Equation, which demonstrates the model of water cloud:

$$B_{sr}^0(\phi) = B_{vr}^0(\phi) + r^2 B_s^0(\phi) \tag{5}$$

$$B_{vr}^0(\phi) = x.w.cos(\phi)\,[1 - r^2(\phi)] \tag{6}$$

$$r^2(\phi) = exp\left[-2y\frac{w}{cos(\phi)}\right] \tag{7}$$

Here $\phi$is the radar incidence angle, $B_{sr}^0(\phi)$ and $B_{vr}^0(\phi)$indicates the surface radar and vegetation layer radar backscattering coefficients, $r^2 B_s^0(\phi)$ indicates the backscattering coefficient of the two-way vegetation radar of the attenuated soil surface, $x$and $y$specifies the corrective value of vegetation moisture content. The mean water content of the vegetation in the pixel is denoted by w and $r^2(\phi)$represents the double-layer attenuation parameter of the radar entering the vegetative layer. The value of the backscattering coefficient with the impact of vegetation removed is given by,

$$B_{vr}^0(\phi) = 0.0009.w.cos\,\phi\left[1 - exp\left(-0.064\frac{w}{cos\,\phi}\right)\right] \tag{8}$$

$$B_s^0(\phi) = \frac{B_{sr}^0(\phi) - 0.0009.w.cos\,\phi\left[1-exp\left(-0.064\frac{w}{cos\,\phi}\right)\right]}{exp\left(-0.064\frac{w}{cos\,\phi}\right)} \tag{9}$$

The backscattering coefficient$B_s^0(\phi)$is then forwarded to the DRN.

3.4. Soil Moisture Retrieval Using DRN

In this section, you will see how the DRN works for extracting soil moisture, as well as its design. It is with the DRN that the retrieval of a soil's moisture is done, where the backscattering coefficient$B_s^0(\phi)$and the vegetative indices obtained $\{v_1, v_2, v_3\}$ are provided as input. The structure of DRN is detailed in the ensuing section.

3.4.1. Structure of DRN

DRN [16] is employed in the process of soil moisture retrieval as it offers minimum error and high accuracy of classification. DRN uses residual blocks, which offer the advantage of connecting the input directly to the output, thereby identifying mapping functions in advance to enhance the performance of the network. The DRN consists of different layers, like the Input, Convolutional (conv), Rectified Linear Activation function (ReLU), Max Pooling, Fully Connected (FC), as well as softmax layers. The backscattering coefficient and the vegetative indices are subjected to the input layer, where 'zero center' normalization is performed.

The convolution layer uses a sequence of kernels or filters to reduce the overall number of free metrics used during training. The max pooling layer reduces the feature size, while the ReLU is used to enhance the nonlinearity in the features. The Fully Connected layer connects all the neurons in the softmax layer to the output of the max pooling layer, converting the scalar probability to soil moisture retrieval. And solving the "vanishing gradient" problem using DRN, DRN unlike less deep networks, contains thousands of convolutional layers.

Increasing the number of neural layers in DRN makes deep neural networks more efficient with less error rate. DRN architecture is illustrated in Figure 2. The deep residual network based "water cloud model "is more capable of managing complex data correlation and non-linearity, lessening vanishing gradient issues as well as enhancing feature abstraction than other methods, such as the K-nearest neighbor technique, thereby demonstrating its robustness in capturing soil moisture accurately.

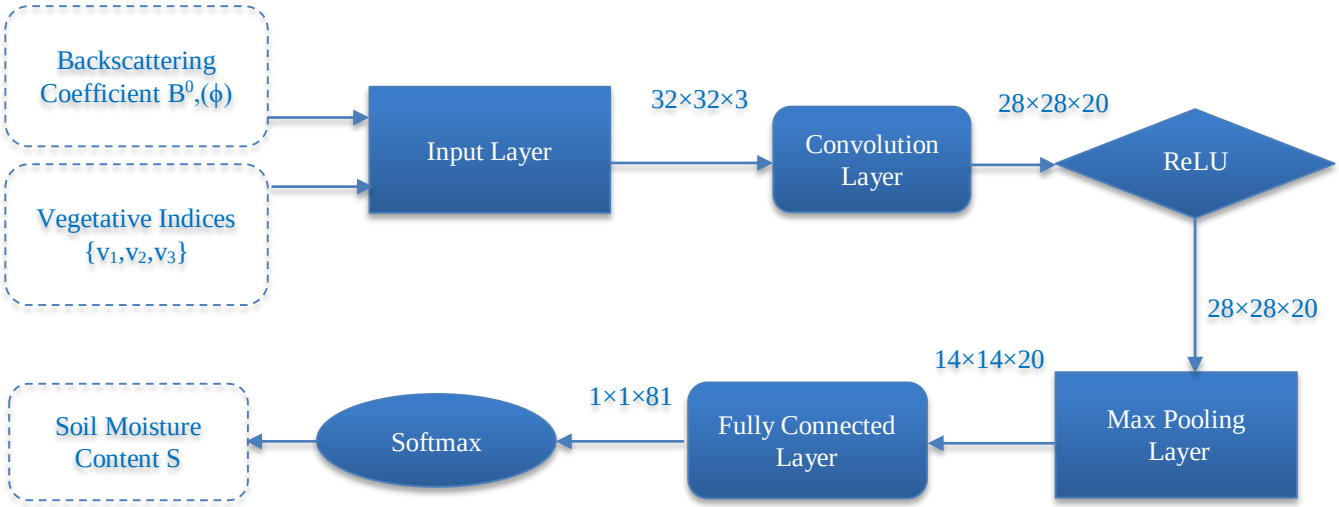

Fig. 2 Architecture of DRN

The output of the DRN *S* gives the amount of soil moisture content.

4. Results and Discussion

The outcomes of the introduced soil moisture estimation technique using a DRN-based water cloud model are detailed in this section. Further, the devised DRN-based water cloud model is evaluated for its performance in comparison to the prevailing approaches.

4.1. Experimental Setup

By employing the proposed method with MATLAB on a system that meets the specified requirements, the produced DRN-based water cloud model is quantitatively evaluated: Windows 10, an Intel i3 processor, and two gigabytes of RAM.

4.2. Dataset Description

The devised DRN-based water cloud model approach is evaluated using the Sentinel-1 dataset [5] and Landsat-8 OLI dataset [6]. The two different data are obtained from Sentinel-1 and Landsat-8 OLI, which are labeled as data-1 and data-2, respectively, and the data is explained below.

i) Data-1:
Site: Amazonas region (Brazil)
Center Latitude 5°47'07.51"S
Center Longitude 68°53'01.57"W

Using the site mentioned overhead, the Landsat-8 OLI data is acquired at row 64, path 3, as well as number 19 and the Sentinel-1 data, is obtained using a relative orbit of 127.

ii) Data-2:
Site: Omsk Oblast region (Russia)
Center Latitude 55°54'40.39"N
Center Longitude 72°03'13.14"E

Using the site mentioned overhead, the Landsat-8 OLI data is acquired at row 21, path 156, and number 2, and the Sentinel-1 data is obtained using a relative orbit of 122.

4.3. Evaluation Metrics

The devised DRN-based water cloud model is analyzed using RMSE and estimation error, and these parameters are detailed below.

4.3.1. Estimation Error

The following equation can be used to represent the estimation error, which is defined as the fraction of standard deviation to the total sample count.

$$e = \frac{\sigma}{\sqrt{n}} \tag{10}$$

Here, n designates the sample count and σ represents the standard deviation.

4.3.2. RMSE

RMSE is the error that is computed between the values predicted and the actual value and is expressed as,

$$R = \frac{\sqrt{\sum_{i=1}^{n}(S_i - S_i^*)^2}}{n} \tag{11}$$

Here, S_i and S_i^* represent the observed and the predicted values of the DRN, respectively.

4.4. Experimental Outcomes

Figure 3 depicts the experimental outcomes of the introduced DRN-based water cloud model with data-1. Figure 3(a) displays the Landsat NIR image, and the Landsat RGB image is depicted using Figure 3(b), Figures 3(c), 3(d), and 3(e) illustrate the veg_GLAI image, veg_SR and veg_WDRVI respectively.

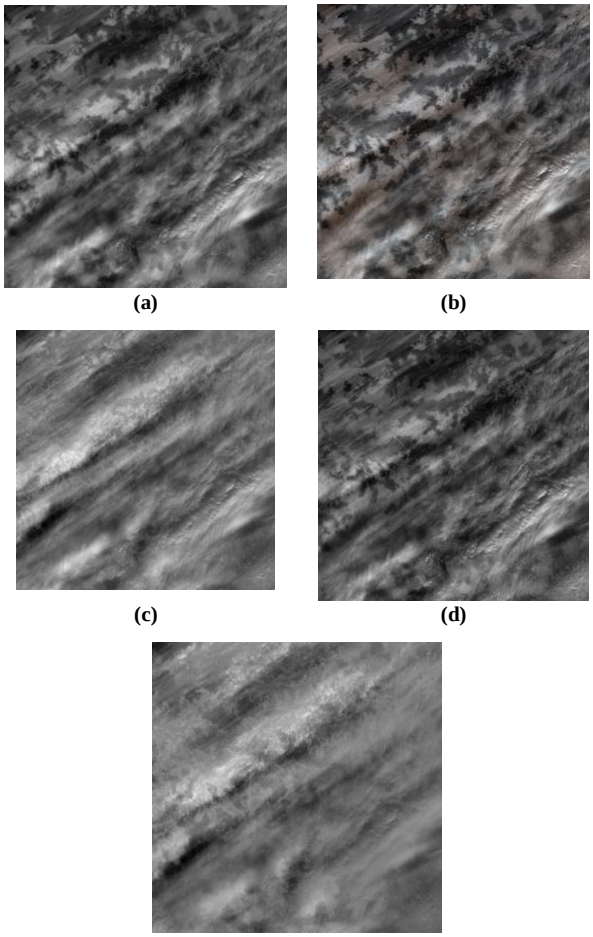

(a) (b) (c) (d) (e)

Fig. 3 Experimental outcomes using data 1, a) Landsat NIR image, b) Landsat RGB image, c) veg_GLAI image, d) veg_SR, and (e) veg_WDRVI.

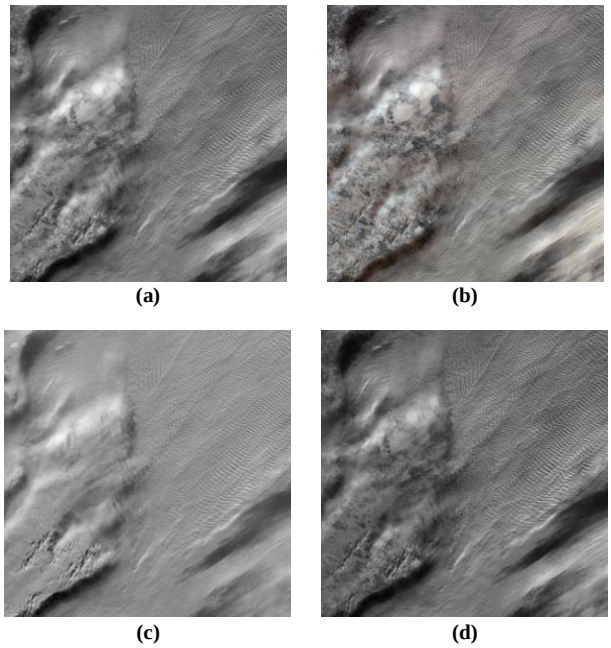

(a) (b) (c) (d)

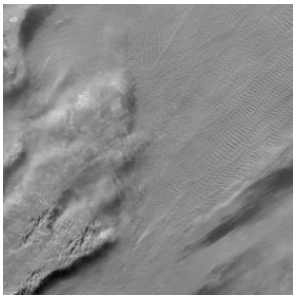

(e)

Fig. 4 Experimental outcomes using data-2, a) Landsat NIR image, (b) Landsat RGB image, (c) veg_GLAI image, (d) veg_SR, and (e) veg_WDRVI.

Figure 4 depicts the experimental results of the devised DNRN based water cloud model using data 1. Figure 4(a) displays the Landsat NIR image 1, the Landsat RGB image is displayed in Figure 4(b), Figure 4(c) depicts the veg_GLAI image, Figures 4(d), and 4(e) illustrates the veg_SR and veg_WDRVI, respectively.

4.5. Comparative Techniques

A detailed analysis of the devised DRN-based water cloud model is carried out in this section to evaluate its performance. The devised technique is compared to the prevailing soil moisture estimation approaches, such as Semi semi-empirical water cloud model [2], Deep multi-model fusion network [3] and the GA technique [1], CNNR [4], and PSO.

4.6. Comparative Evaluation

Metrics like estimation error and RMSE are used to assess the performance of the developed DRN-based water cloud model using data 1 and data 2, with varying numbers of training samples taken into account.

4.6.1. Evaluation with Data 1

Figure 5 depicts the assessment of the devised DRN-based water cloud model using data 1. In Figure 5(a), the analysis is depicted based on estimation error. The estimation error computed by the Semi-empirical water cloud model, Deep multi model fusion network, GA technique, CNNR, and PSO is 9.657, 1.815, 7.056, 1.706, and 6.633, whereas the devised DRN-based water cloud model computed a less value of estimation error at 0.851 while considering 70 training samples.

Figure 5(b) depicts the RMSE based evaluation. The proposed DRN-based water cloud model computed an RMSE of 1.017 when 80 samples were taken into account. This is less than the RMSE values of 2.586, 11.002, 7.547, 10.342, and 7.095 computed by the existing techniques, such as the Deep Multi Model Fusion Network, GA, CNNR, and PSO, and the Semi Empirical Water Cloud Model.

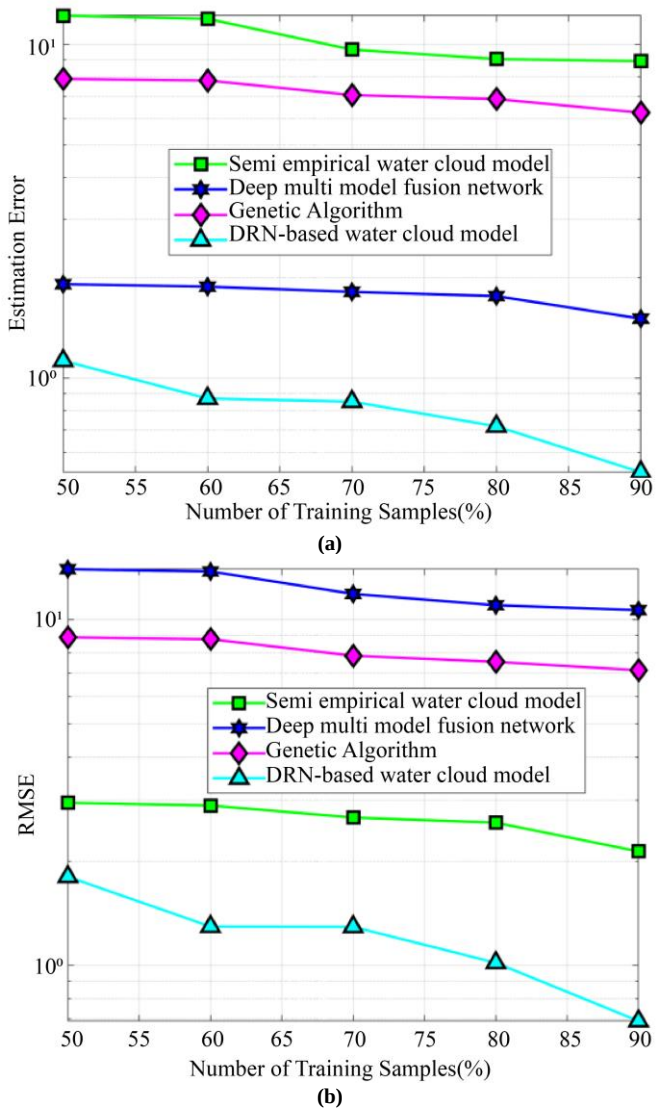

Fig. 5 Assessment of the devised DRN- based water cloud model using data-1 based on (a) estimation error, and (b) RMSE.

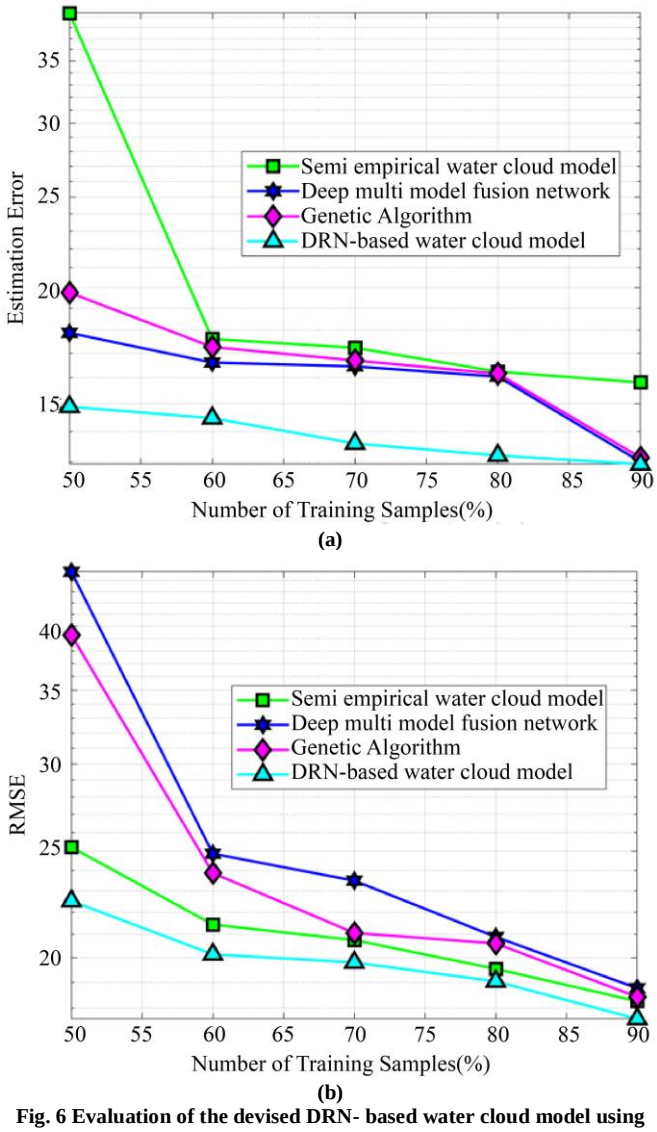

Fig. 6 Evaluation of the devised DRN- based water cloud model using data 2 based on (a) Estimation error, (b) RMSE.

4.6.2. Evaluation Using Data 2

In Figure 6, the evaluation of the devised DRN-based water cloud model for soil moisture estimation is depicted. Figure 6(a) illustrates the analysis using estimation error. For 60 samples, the value of estimation error computed by the proposed DRN-based water cloud model is 14.479, whereas the existing methods computed a higher value of estimation error, with 17.608 for Semi empirical water cloud model, 16.612 for Deep multi model fusion network, 17.264 for GA, CNNR for 15.615, and PSO for 16.229. The evaluation using RMSE is displayed in Figure 6(b). The value of RMSE computed by the Semi empirical water cloud model, Deep multi model fusion network, GA, CNNR, PSO, and the devised DRN-based water cloud model is 25.205, 44.810, 39.263, 42.121, 36.907, and 22.524 for 50 samples, which reveals that the value computed by the proposed method is better.

5. Results

In Figure 6, the evaluation of the devised DRN-based water cloud model for soil moisture estimation is depicted. Figure 6(a) illustrates the analysis using estimation error. For 60 samples, the value of estimation error computed by the proposed DRN-based water cloud model is 14.479, whereas the existing methods computed a higher value of estimation error, with 17.608 for Semi empirical water cloud model, 16.612 for Deep multi model fusion network, 17.264 for GA, CNNR for 15.615, and PSO for 16.229. The evaluation using RMSE is displayed in Figure 6(b). The value of RMSE computed by the Semi empirical water cloud model, Deep multi model fusion network, GA, CNNR, PSO, and the devised DRN-based water cloud model is 25.205, 44.810, 39.263, 42.121, 36.907, and 22.524 for 50 samples, which reveals that the value computed by the proposed method is better.

Table 1. Comparative discussion

Satellite Data	Parameters	Semi Empirical Water Cloud Model	Deep Multi Model Fusion Network	GA	Proposed DRN-based Water Cloud Model
Data-1	Estimation Error	8.922	1.508	6.249	**0.523**
	RME	2.135	10.649	7.137	**0.690**
Data-2	Estimation Error	15.814	13.000	13.137	12.920
	RME	18.266	18.772	18.433	17.608

6. Conclusion

Soil moisture is a key factor impacting the productivity and growth of plants. Moreover, it is a major factor affecting the hydrological cycle that exists between the soil surface and the atmosphere. Determining the moisture content of the soil is crucial since it helps determine whether irrigation is necessary beforehand. Here, a unique method for retrieving soil moisture that is based on the water cloud model is created. The estimation of soil moisture retrieval is done using satellite photos. Vegetation indices, including GLAI, SR, and WDRVI, are derived from the photos, and the water cloud model estimates the backscatter coefficient.

These parameters are then subjected to the DRN, where soil moisture retrieval is performed. The devised approach is essential in monitoring the growth of crops and their yields and providing food security. Further, the introduced DRN-based water cloud model is evaluated for its performance using metrics, such as estimation error and RMSE, and is found to have attained a minimal value of estimation error and RMSE as 0.523 and 0.69, respectively, which reveals superior performance. The future focus will be to enhance the performance of the technique by considering more vegetation indices and utilization of other deep learning networks. Also, more evaluation metrics will be considered for the performance evaluation.

Compared to previous approaches, the Deep Residual Network (DRN)-based water cloud model performs better because it can manage complex data correlations and nonlinearity. The DRN architecture's residual blocks and several layers effectively reduce the vanishing gradient issue and enhance feature extraction. The addition of vegetation indicators such as GLAI, SR, and WDRVI improves the model's estimation of soil moisture accuracy. In comparison to methods such as the Semi-Empirical Water Cloud Model, Deep Multi-Model Fusion Network, GA, CNNR, and PSO, our model achieves reduced RMSE and estimate error, suggesting its robustness and effectiveness in properly capturing soil moisture dynamics.

References

[1] Kamal Kumar, K.S. Hari Prasad, and M.K. Arora, "Estimation of Water Cloud Model Vegetation Parameters Using a Genetic Algorithm," *Hydrological Sciences Journal*, vol. 57, no. 4, pp. 776-789, 2012. [CrossRef] [Google Scholar] [Publisher Link]

[2] S. Said, U.C. Kothyari, and M.K. Arora, "Vegetation Effects on Soil Moisture Estimation from ERS-2 SAR Images," *Hydrological Sciences Journal*, vol. 57, no. 3, pp. 517-534, 2012. [CrossRef] [Google Scholar] [Publisher Link]

[3] Grigorios Tsagkatakis, Mahta Moghaddam, and Panagiotis Tsakalides, "Deep Multi-Modal Satellite and in-Situ Observation Fusion for Soil Moisture Retrieval," *2021 IEEE International Geoscience and Remote Sensing Symposium IGARSS*, Brussels, Belgium, pp. 6339-6342, 2021. [CrossRef] [Google Scholar] [Publisher Link]

[4] Jian Liu et al., "Soil Moisture Retrieval in Farmland Areas with Sentinel Multi-Source Data Based on Regression Convolutional Neural Networks," *Sensors*, vol. 21, no. 3, pp. 1-21, 2021. [CrossRef] [Google Scholar] [Publisher Link]

[5] Sentinel-1 Dataset. [Online]. Available: https://scihub.copernicus.eu/dhus/#/home

[6] Landsat-8 OLI Dataset. [Online]. Available: https://earthexplorer.usgs.gov/

[7] Sonia I. Seneviratne et al., "Investigating Soil Moisture–Climate Interactions in A Changing Climate: A Review," *Earth-Science Reviews*, vol. 99, no. 3-4, pp. 125-161, 2010. [CrossRef] [Google Scholar] [Publisher Link]

[8] Kaighin A. McColl et al., "The Global Distribution and Dynamics of Surface Soil Moisture," *Nature Geoscience*, vol. 10, no. 2, pp. 100-104, 2017. [CrossRef] [Google Scholar] [Publisher Link]

[9] S.U. Susha Lekshmi, D.N. Singh, and Maryam Shojaei Baghini, "A Critical Review of Soil Moisture Measurement," *Measurement*, vol. 54, pp. 92-105, 2014. [CrossRef] [Google Scholar] [Publisher Link]

[10] Venkat Lakshmi, "Remote Sensing of Soil Moisture," *International Scholarly Research Notices*, 2013. [CrossRef] [Google Scholar] [Publisher Link]

[11] Prashant K. Srivastava, "Satellite Soil Moisture: Review of Theory and Applications in Water Resources," *Water Resources Management*, vol. 31, no. 10, pp. 3161-3176, 2017. [CrossRef] [Google Scholar] [Publisher Link]

[12] Jian Peng et al., "Spatial Downscaling of Satellite Soil Moisture Data Using a Vegetation Temperature Condition Index," *IEEE Transactions on Geoscience and Remote Sensing*, vol. 54, no. 1, pp. 558-566, 2015. [CrossRef] [Google Scholar] [Publisher Link]

[13] M.E. Holzman, R. Rivas, and M.C. Piccolo, "Estimating Soil Moisture and the Relationship with Crop Yield Using Surface Temperature and Vegetation Index," *International Journal of Applied Earth Observation and Geoinformation*, vol. 28, pp. 181-192, 2014. [CrossRef] [Google Scholar] [Publisher Link]

[14] A. Bannari et al., "A Review of Vegetation Indices," *Remote Sensing Reviews*, vol. 13, no. 1-2, pp. 95-120, 1995. [CrossRef] [Google Scholar] [Publisher Link]

[15] Emmanouil Psomiadis et al., "The Role of Spatial and Spectral Resolution on the Effectiveness of Satellite-Based Vegetation Indices," *Remote Sensing for Agriculture, Ecosystems, and Hydrology XVIII*, vol. 9998, pp. 509-521, 2016. [CrossRef] [Google Scholar] [Publisher Link]

[16] Ali Ben Abbes, Ramata Magagi, and Kalifa Goita, "Soil Moisture Estimation from Smap Observations Using Long Short-Term Memory (LSTM)," *IGARSS 2019 - 2019 IEEE International Geoscience and Remote Sensing Symposium*, Yokohama, Japan, pp. 1590-1593, 2019. [CrossRef] [Google Scholar] [Publisher Link]

[17] Shuai Huang et al., "Soil Moisture Retrival Based on Sentinel-1 Imagery under Sparse Vegetation Coverage," *Sensors*, vol. 19, no. 3, pp. 1-18, 2019. [CrossRef] [Google Scholar] [Publisher Link]

[18] Zhicong Chen et al., "Deep Residual Network-Based Fault Detection and Diagnosis of Photovoltaic Arrays Using Current-Voltage Curves and Ambient Conditions," *Energy Conversion and Management*, vol. 198, 2019. [CrossRef] [Google Scholar] [Publisher Link]

[19] Anil B. Gavade, and Vijay S. Rajpurohit, "Sparse-FCM and Deep Learning for Effective Classification of Land Area in Multi-Spectral Satellite Images," *Evolutionary Intelligence*, pp. 1-17, 2020. [CrossRef] [Google Scholar] [Publisher Link]

[20] Abhilash Singh et al., "Comparison of Different Dielectric Models to Estimate Penetration Depth of L-and S-Band SAR Signals Into the Ground Surface," *Geographies*, vol. 2, no. 4, pp. 734-742, 2022. [CrossRef] [Google Scholar] [Publisher Link]

[21] Prabhjot Kaur et al., "A Novel Transfer Deep Learning Method for Detection and Classification of Plant Leaf Disease," *Journal of Ambient Intelligence and Humanized Computing*, vol. 14, pp. 12407-12424, 2022. [CrossRef] [Google Scholar] [Publisher Link]

[22] Sijia Hao et al., "Model-Based Mechanism Analysis of "7.20" Flash Flood Disaster in Wangzongdian River Basin," *Water*, vol. 15, no. 2, pp. 1-15, 2023. [CrossRef] [Google Scholar] [Publisher Link]

[23] Mukund Pratap Singh, and Pitam Singh, "Multi-Criteria GIS Modeling for Optimum Route Alignment Planning in Outer Region of Allahabad City, India," *Arabian Journal of Geosciences*, vol. 10, 2017. [CrossRef] [Google Scholar] [Publisher Link]

[24] Mukund Pratap Singh, Pitam Singh, and Priyamvada Singh, "Fuzzy AHP-Based Multi-Criteria Decision-Making Analysis for Route Alignment Planning Using Geographic Information System (GIS)," *Journal of Geographical Systems*, vol. 21, pp. 395-432, 2019. [CrossRef] [Google Scholar] [Publisher Link]

[25] Zhenghua Huang et al., "D^3CNNs: Dual Denoiser Driven Convolutional Neural Networks for Mixed Noise Removal in Remotely Sensed Images," *Remote Sensing*, vol. 15, no. 2, pp. 1-20, 2023. [CrossRef] [Google Scholar] [Publisher Link]

[26] Abhilash Singh et al., "A Deep Learning Approach to Predict the Number of K-Barriers for Intrusion Detection over a Circular Region Using Wireless Sensor Networks," *Expert Systems with Applications*, vol. 211, 2023. [CrossRef] [Google Scholar] [Publisher Link]

[27] Mohsen Jamali et al., "Wheat Leaf Traits Monitoring Based on Machine Learning Algorithms and High-Resolution Satellite Imagery," *Ecological Informatics*, vol. 74, 2023. [CrossRef] [Google Scholar] [Publisher Link]

[28] M. Lavreniuk et al., "Reviewing Deep Learning Methods in the Applied Problems of Economic Monitoring Based on Geospatial Data," *Cybernetics and Systems Analysis*, vol. 58, pp. 1008-1020, 2022. [CrossRef] [Google Scholar] [Publisher Link]

[29] Yanling Wang et al., "A Comprehensive Study of Deep Learning for Soil Moisture Prediction," *Hydrology and Earth System Sciences*, vol. 28, no. 4, pp. 917-943, 2024. [CrossRef] [Google Scholar] [Publisher Link]

[30] Rong Fu et al., "A Soil Moisture Prediction Model, Based on Depth and Water Balance Equation: A Case Study of the Xilingol League Grassland," *International Journal of Environmental Research and Public Health*, vol. 20, no. 2, pp. 1-18, 2023. [CrossRef] [Google Scholar] [Publisher Link]

[31] Abhilash Singh, and Kumar Gaurav, "Deep Learning and Data Fusion to Estimate Surface Soil Moisture from Multi-Sensor Satellite Images," *Scientific Reports*, vol. 13, pp. 1-20, 2023. [CrossRef] [Google Scholar] [Publisher Link]